Features of the Reaction $\pi^+d \to \pi^+d\pi^+\pi^-$ at 4.2 GeV/c†

B. EISENSTEIN AND H. GORDON
Department of Physics, University of Illinois, Urbana, Illinois 61801
(Received 2 September 1969)

Prominent features of this reaction include d^* production in the $d\pi^+$ system, ρ^0 production, and a low-mass enhancement (A_1) in the $\rho^0\pi^+$ system. A model for πd scattering has been found to provide an adequate description of the properties of the d^*. A Reggeized pion-exchange model successfully predicts the properties of the $\rho^0\pi^+d$ final state, whether or not d^* formation occurs.

I. INTRODUCTION

IN this paper we present a study of the reaction

$$\pi^+d \to \pi^+d\pi^+\pi^- \tag{1}$$

at 4.19 GeV/c. The data were obtained in an experiment employing the Lawrence Radiation Laboratory 72-in. deuterium bubble chamber. Details are presented in Sec. II. Previous studies of this reaction[1–4] have been concerned with the d^* effect in the πd system and with the search for the production off the deuteron of a meson decaying into three pions.

In Sec. III we show that the features of the d^* system agree with a simple model in which πd elastic scattering proceeds via a nucleon-$\Delta(1238)$ intermediate state. In Sec. IV we present a comparison of the features of the $\rho^0\pi^+$ events with the predictions of a Reggeized pion-exchange calculation. As would be expected, the data containing only d^* events are in excellent agreement with the model. Moreover, the non-d^* data also are consistent with the calculation.

II. DATA ANALYSIS AND EVENT SELECTION

The events presented here are drawn from about 21 000 four-prong events measured with the Illinois SMP system. The sample includes only events which contained at least one stopping track whose momentum is greater than 130 MeV/c. Candidates for reaction (1) were selected on the basis of χ^2 probability for a four-constraint fit. Our final sample of data is composed of 696 events. In addition to the requirement that reaction (1) be the fit with highest χ^2 probability, we also require that bubble density information from the fit correspond to the event examined on the scanning table.

The chief competitor to the fit to hypothesis (1) is the one-constraint fit to

$$\pi^+d \to \pi^+pn\pi^+\pi^-, \tag{2}$$

where the final-state proton is a low-momentum spectator to the strong interaction. A study similar to those reported previously[5] indicates that there is little contamination in our sample. In fact, we estimate that about 70 events which were actually cases of reaction (1) were misassigned by our criteria to reaction (2). After studying their properties, we believe that the exclusion of these events from our sample does not alter any of our conclusions.

The total cross section for reaction (1) is 275 ± 60 μb. This cross section has been corrected for the events misassigned to reaction (2), and also for a small percentage of poorly measured events which had a three-constraint fit to (1). The large error reflects an uncertainty in the total path length which is due to a large ($\approx 18\%$) proton contamination in the pion beam, besides including the uncertainty in the above corrections. We have not increased the cross section to include cases of reaction (1) where the deuteron either did not stop or was too short to leave a visible track. Only the second effect should be significant, and a preliminary analysis of three-prong events suggests that the increase in cross section should be no greater than 10%.

For the purpose of presenting our data, we have further restricted our events to those whose χ^2 probability is $\geq 2\%$, although the inclusion of the others would not appreciably change any conclusions. The following analysis is based, then, on the 624 remaining events.

III. ρ^0 AND d^* PRODUCTION

In Fig. 1 are shown the $d\pi$ and $\pi^+\pi^-$ invariant-mass distributions. Both the low-mass $d\pi^+$ enhancement (d^{*++}) and the ρ^0 signal are quite prominent, even though Figs. 1(a) and 1(b) contain two combinations per event. Following the procedure introduced in Ref. 4, for each event we define π_2^+ as the member of the $\pi^+\pi^-$ combination which is produced with smaller four-momentum transfer squared from the beam pion. The remaining positive pion is labelled π_1^+. We define a ρ band as 0.665 to 0.865 GeV/c^2, and a d^* band as 2.0 to 2.4 GeV/c^2. We see in Fig. 1(a) that the d^{*++} is produced almost exclusively as a $d\pi_1^+$ combination, and that in Fig. 1(b) the ρ^0 is produced predominantly as a $\pi_2^+\pi^-$ pair. Hereafter, d^{*++} events will refer to $d\pi_1^+$ pairs. Although ρ's containing π_2^+ appear to have

† Work supported in part by the U. S. Atomic Energy Commission.

[1] A. M. Cnops *et al.*, Phys. Rev. Letters **21**, 1609 (1968).
[2] G. Vegni *et al.*, Phys. Letters **19**, 526 (1965).
[3] A. Forino *et al.*, Phys. Letters **19**, 68 (1965).
[4] M. A. Abolins *et al.*, Phys. Rev. Letters **15**, 125 (1965).

[5] The study included a check of m_{pn} and $\cos\theta_{pn}$ for the competing $pn\pi^+\pi^+\pi^-$ fits, as described in Ref. 3.

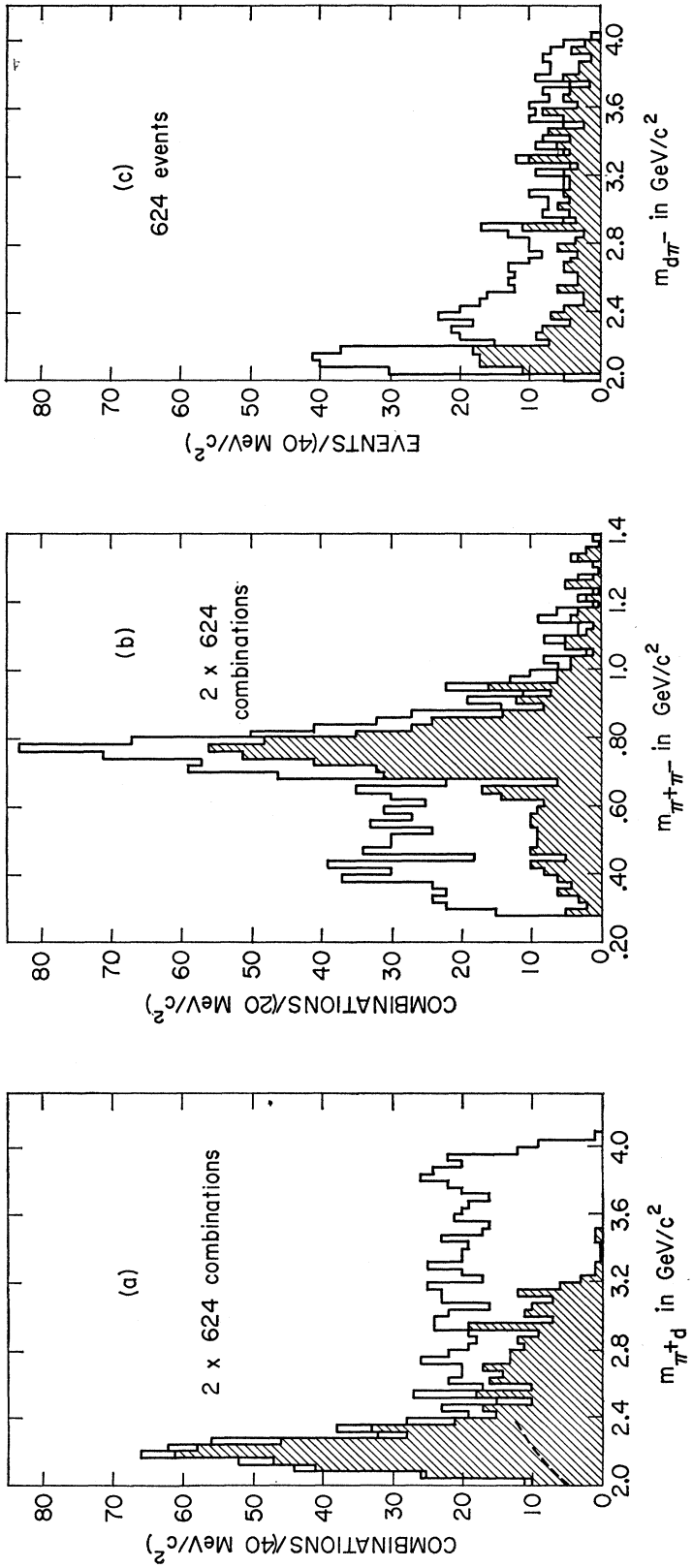

FIG. 1. (a) Mass of $d\pi^+$. Shaded region represents $d\pi_1^+$ events only. Dashed line represents estimate of background in $d\pi_1^+$. (b) Mass of $\pi^+\pi^-$. Shaded region represents $\pi_2^+\pi^-$ events only. (c) Mass of $d\pi^-$. Shaded region represents events for which $\pi_2^+\pi^-$ is not in ρ^0 band.

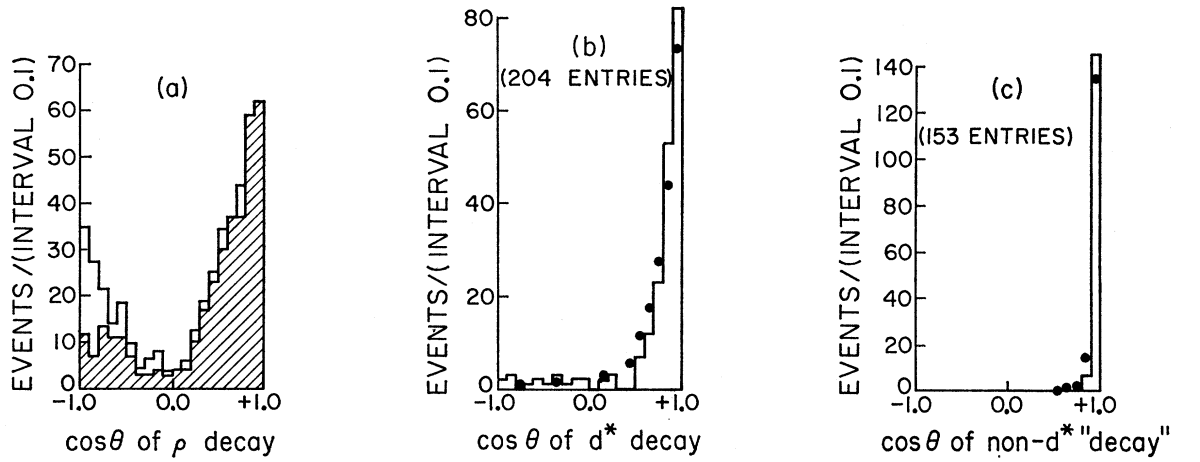

FIG. 2. (a) Polar angle of π^+ from ρ^0 decay. For the unshaded histogram, a ρ^0 was defined as any $\pi^+\pi^-$ whose mass lay in ρ^0 band. Contributions from events with double ρ's were each weighted by $\frac{1}{2}$. Shaded region represents 357 events where $\pi_2{}^+\pi^-$ was in ρ^0 band. (b) Polar angle of deuteron from d^* decays in events containing ρ^0's. Dots are from Regge model described in Sec. IV. (c) Polar angle of deuteron in $d\pi_1{}^+$ system for non-d^* events containing ρ^0's. Dots are from Regge model in Sec. IV.

little background, we note that this method of selection preferentially excludes not only those ρ's produced with large momentum transfers, but also those ρ's which decay so that their π^+ moves backwards with respect to the ρ^0 line of flight. This latter exclusion enhances the observed asymmetry in the ρ decay when only $\pi_2{}^+\pi^-$ pairs are considered, as displayed in Fig. 2(a). We estimate that 10% of all ρ's in the data are excluded by this cut.

Although a low-mass enhancement is seen in the $d\pi^-$ system in Fig. 1(c), when events containing a $\rho^0(\pi_2{}^+)$ are excluded only a small bump remains apparent. The further exclusion of the ρ^0 band in $\pi_1{}^+\pi^-$ pairs or of d^{*++} events produces a featureless $d\pi^-$ mass spectrum. We conclude that d^{*0} production, if present at all, is very small, and that the observed enhancement results primarily from reflections of the ρ^0 or d^{*++} decays.

It has already been observed[4] that the d^* enhancement should not be interpreted as evidence for a resonant particle. In Fig. 2(b) we show the "decay" angular distribution of the d^{*++} events produced with a ρ^0. The angle θ is between the incoming and outgoing deuterons in the d^* rest frame. This asymmetric distribution cannot result from the strong decay of a particle with definite spin and parity. For comparison, Fig. 2(c) shows the corresponding angular distribution for $d\pi_1{}^+$ pairs whose mass is greater than 2.4 GeV/c^2 (called hereafter non-d^* events). In both cases the associated azimuthal distribution is quite isotropic.

The d^* has been assumed to be an enhancement in πd scattering which results from the formation of a $\Delta(1238)$ by one of the nucleons in the deuteron. The Δ subsequently decays in a way which leaves an intact deuteron in the final state. The simplest support for this hypothesis is the observation that the d^* mass is very nearly equal to the sum of the Δ and nucleon masses.

A possible mechanism for d^* production is illustrated by the Feynman diagram of Fig. 3(b). We note that the ρ^0 decay angular distribution for $\rho^0 d^*$ events (not shown) is similar to the unshaded histogram in Fig. 2(a), suggesting that the ρ's are produced by pion exchange.[6]

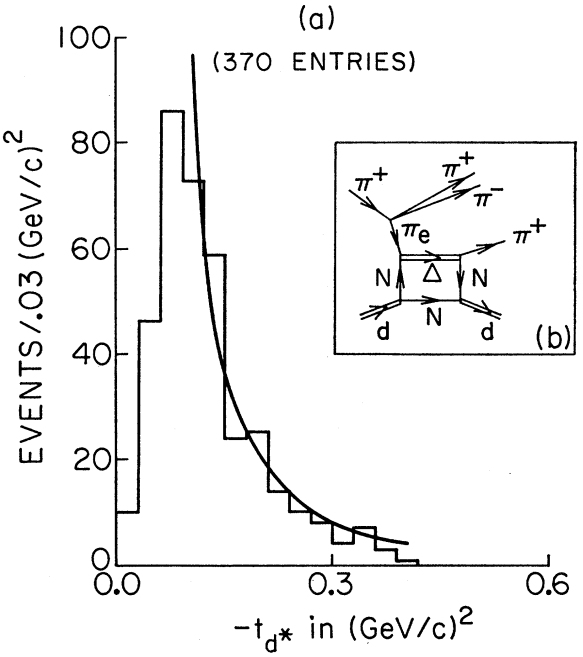

FIG. 3. (a) Momentum transfer from deuteron to d^*. Curve is pion propagator. (b) Box diagram for production of d^* events.

[6] We have analyzed the ρ^0 decay angular distributions for both d^* and non-d^* events in terms of a 1^- meson interfering with a 0^+ background, as in R. L. Eisner *et al.*, Phys. Rev. 164, 1699 (1967). In order to minimize biases in the angular distributions, the ρ^0 events were selected only on the basis of mass cuts. We find $\rho_{00}-\rho_{11}=0.68$, for events with or without d^*'s. Such a large value is suggestive of π exchange in the production process.

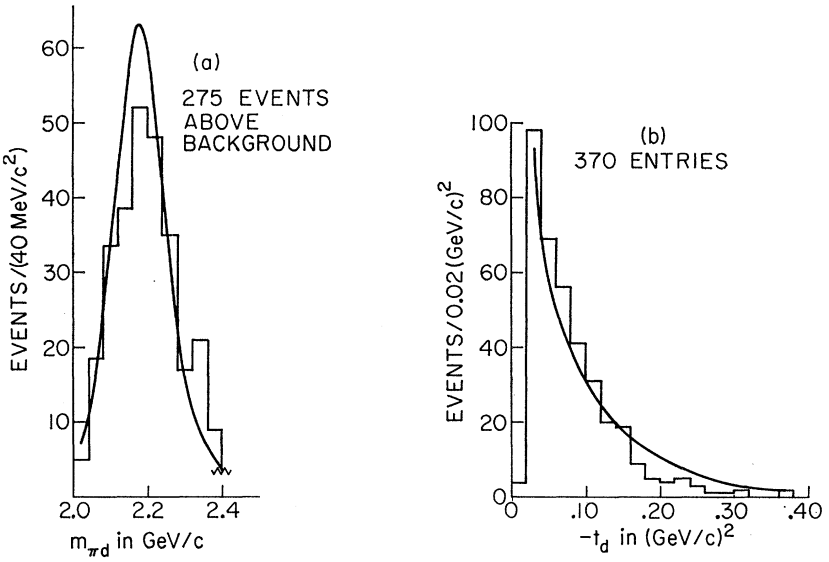

FIG. 4. (a) Mass of $d\pi_1^+$ in d^* region above background estimate shown in Fig. 1(a). Curve is from box calculation scaled to number of events. (b) Momentum transfer from deuteron to deuteron in d^* events. Curve is from box calculation scaled to number of events.

As further evidence that the reaction

$$\pi^+ d \rightarrow \pi^+\pi^- d^{*++} \tag{3}$$

proceeds via pion exchange, in Fig. 3(a) we show the distribution of t_{d^*}, the square of the four-momentum transfer from the incident deuteron to the d^{*++}. (The dip near $t=0$ reflects the fact that for some events $t_{\min}$ can be quite large.) The superimposed curve represents a pion propagator $1/(t_{d^*}-m_\pi^2)^2$, normalized to the data between -0.12 and -0.42 (GeV/c)^2. It is interesting to note how well it reproduces the observed t_{d^*} distribution.

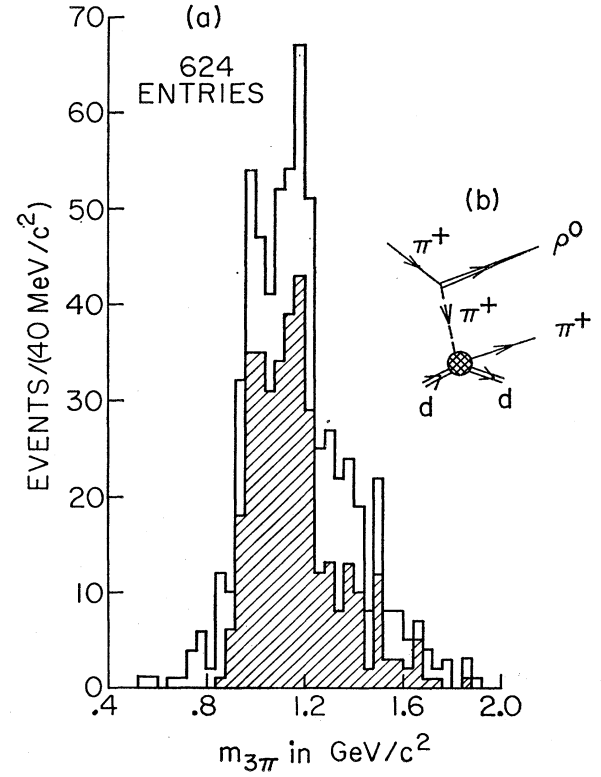

FIG. 5. (a) Three-pion mass for all events. Shaded region represents 357 events for which $\pi_2^+\pi^-$ is in ρ^0 band. (b) Diagram for production of $\rho^0\pi^+ d$ final state.

A box graph similar to the lower part of Fig. 3(a) was evaluated by Month[7] for the process $\gamma d \rightarrow \gamma d$. It leads to a cross section which peaks in the neighborhood of 2.2 GeV/c^2, but does not correspond to a resonance in any single partial wave. We have modified Month's calculation to include the nonzero pion mass, but to simplify matters we have ignored spin at the upper vertex and have treated the exchanged pion as if it were real. Month's calculation, although relativistic, ignores spin effects and uses only the deuteron binding energy to evaluate the dNN couplings.

Following Pilkuhn,[8] we write

$$\frac{d^2\sigma}{dm_{d^*}dt_d} = \frac{m_{d^*}|B(m_{d^*}^2,t_d)|^2}{[(m_{d^*}^2-m_d^2-m_\pi^2)^2-4m_d^2m_\pi^2]^{1/2}}G, \tag{4}$$

[7] M. Month, Phys. Rev. **155**, 1689 (1967).

[8] H. Pilkuhn, *The Interaction of Hadrons* (North-Holland Publishing Co., Amsterdam, 1967). We use the peripheral-model formalism described on pp. 279–280. From his Eqs. (2.2) and (2.3), the cross section for the process depicted in our Fig. 3(b) is

$$\frac{d^3\sigma}{dt dm_{\pi\pi}^2 dm_{d^*}^2} \propto \frac{[\lambda(m_{\pi\pi}^2,m_\pi^2,t)]^{1/2}\sigma(\pi+\pi\rightarrow\pi+\pi) \times[\lambda(m_{d^*}^2,m_d^2,t)]^{1/2}\sigma(\pi+d\rightarrow\pi+d)}{(m_\pi^2-t)^2},$$

where t is the four-momentum squared of the exchanged pion (π_e) and $\lambda(a,b,c)=(a-b-c)^2-4bc$. We note experimentally that the d^* properties do not depend markedly on $m_{\pi\pi}$, so we "decouple" the upper and lower vertices by replacing the pion propagator with $\delta(m_\pi^2-t)$. After integration we have $d\sigma/dm_{d^*}^2 \propto [\lambda(m_{d^*}^2,m_d^2,m_\pi^2)]^{1/2}\sigma(\pi d\rightarrow\pi d)$. We further assume that this relation holds in differential form as $d^2\sigma/dm_{d^*}^2dt_d \propto (\sqrt{\lambda})d\sigma(\pi d)/dt_d$, where t_d is defined in the text. From Month's expression for $(d\sigma/d\Omega)_{\text{c.m.}}$ for real πd scattering via a box diagram, we write $d\sigma(\pi d)dt_d \propto |B(m_{d^*}^2,t_d)|^2/\lambda(m_{d^*}^2,m_d^2,m_\pi^2)$, and substitute this into the previous expression to arrive at our Eq. (4) (where for convenience we use dm_{d^*} rather than $dm_{d^*}^2$).

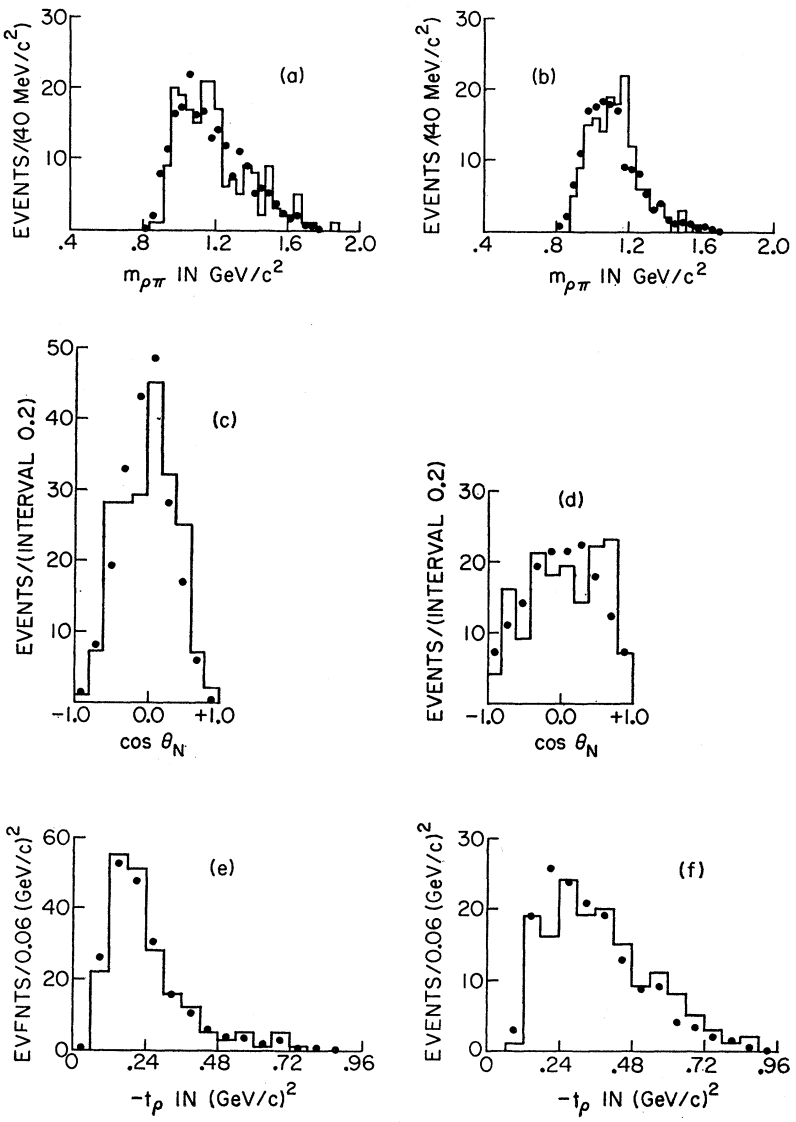

FIG. 6. Features of $\rho^0\pi_1{}^+d$ final state. Diagrams (a), (c), and (e) contain 204 d^* events, while (b), (d), and (f) contain 153 non-d^* events. The dots are predictions of the Regge model. (a) and (b) Mass of $\rho\pi$. (c) and (d) Polar angle of "decay normal" of $\rho\pi$ system. (e) and (f) Momentum transfer from beam pion to ρ^0.

where B is the amplitude for the box,[7] t_d is the square of the four-momentum transfer between incoming and outgoing deuterons, and G represents a normalization which we determine experimentally. In (4) we have already put the exchanged pion on its mass shell and suppressed the dependence of the cross section on $m_{\pi\pi}$, the mass of the outgoing pion pair at the upper vertex.

In Fig. 4(a) we show the d^{*++} mass distribution remaining after subtraction of the background estimate given by the broken line in Fig. 1(a). The superimposed curve represents the result of integrating (4) over t_d from -0.03 to -0.33 $(\mathrm{GeV}/c)^2$, and of fixing G to arrive at the same number of events as in the data. The agreement is quite satisfactory.

Figure 4(b) shows the distribution of t_d for the d^{*++} events. The curve represents the result of integrating (4) over m_{d^*} from 2.04 to 2.40 GeV/c^2. The same value of G was used, but an adjustment in scale was made since no background was subtracted here. The agreement is adequate, but we observe that the data do fall off more rapidly with t_d than the theory predicts. It is perhaps surprising that the model works as well as it does, because it contains no information about deuteron structure other than the binding energy. We might expect that the inclusion of more detailed information (that contained in the short-range term in the Hulthén wave function, for example) would improve the agreement with the observed t_d distribution.

IV. $\rho^0\pi^+$ SYSTEM

The invariant mass of the three outgoing pions for all 624 events is shown in Fig. 5(a). Also shown is the distribution resulting from the inclusion of only those

events containing a ρ^0. In this section, only $\pi_2^+\pi^-$ pairs are candidates for a ρ^0. As we saw in Fig. 1(b), this allows a selection of a ρ^0 sample that is free from background, although we must be careful to take into account the biases inherent in this scheme.

Both graphs display a low-mass enhancement about 300 MeV/c^2 wide and centered at about 1.1 GeV/c^2. There is no evidence for narrow resonances within the large peak, which for convenience we refer to as the A_1 meson. Furthermore, the 3π mass distribution remaining when all ρ^0's are excluded (not shown) has no striking features and is both broader and much less peaked. In the following discussions we have, for simplicity, limited ourselves to the $\rho^0\pi^+d$ final state.

It is natural to inquire whether the A_1 may be interpreted as a kinematic enhancement. We might anticipate the validity of that interpretation for the A_1 in the ρ^0d^* events, where we believe the production takes place in the manner sketched in Fig. 5(b). [In contrast to Fig. 3(b), here we suppress details of the πd scattering.] Separate studies of the final states ρ^0d^* and $\rho^0\pi^+d$ (non-d^*) have therefore been made.

In Figs. 6(a) and 6(b) we show the $\rho\pi$ mass for d^* and non-d^* events. The distributions are similar except for a relative excess of events in the region from 1.2 to 1.6 GeV/c^2 in the case of d^*'s. Figures 6(c) and 6(d) illustrate the A_1 decay angular distribution. Since most of the events in the $\rho\pi$ mass spectra concentrate at low masses, we have not bothered to define an A_1 mass band in plotting these angular distributions, but rather have included all $\rho\pi$ events. The angle θ is between the normal to the $\pi^+\pi^+\pi^-$ plane and the beam pion in the $\rho^0\pi^+$ rest frame. These distributions are markedly different for d^* and non-d^* events, but both bear some characteristic similarity to a $\sin^2\theta$ distribution. The corresponding azimuthal distributions (not shown) are reasonably isotropic. Finally, in Figs. 6(e) and 6(f) we show the distributions of t_ρ, the momentum transfer between the beam pion and the ρ^0.

We have calculated the above distributions using the Regge-pole exchange model introduced by Berger.[9] We have employed a pion trajectory of the form $\alpha(t_\rho)=t_\rho-m_\pi^2$ and the $\rho\pi\pi$ coupling specified in the reference. In the Monte Carlo calculation the ρ is treated as a particle of zero width, but the ρ mass is varied for each event according to a Breit-Wigner distribution. The πd scattering is represented by the on-shell cross section which is assumed proportional to e^{At_d}. We find A by fitting the t_d distributions between $t_d=-0.03$ and -0.23 (GeV/c)^2 and obtain $A_{d^*}=16.8$ (GeV/c)$^{-2}$ and $A_{\text{non-}d^*}=20.5$ (GeV/c)$^{-2}$.

There is insufficient published data on πd total cross sections in the range of πd invariant mass from 2.2 to 3.6 GeV/c^2 to permit an absolute normalization to be calculated. Instead, we have assumed that the features of interest in the $\rho\pi d$ system are insensitive to the size of the πd cross section and have simply generated a number of events for each sample (d^* and non-d^*) proportional to the number occurring in the data.

Since the model does not predict the ρ^0 density matrix, we have generated the events so that $\rho_{00}=1$ and all other elements are zero.[10]

The Monte Carlo events are then subjected to the same cuts (and biases) as the data. In particular, when we graph the predictions we suppress the knowledge of which π^+ is actually the bachelor pion, and we select ρ's and d^*'s (or non-d^*'s) on the basis of mass cuts and the π_1^+, π_2^+ test. In order to compare the model to our data, we have scaled the predictions to correspond to 204 d^* events and 153 non-d^* events.

The Monte Carlo predictions are shown by the dots in Figs. 2(b), 2(c), and 6(a)–6(f). The $d\pi_1^+$, $\rho^0\pi_1^+$, and t_ρ distributions agree quite well with the model. Other distributions (not shown), such as the azimuth of the $\rho\pi$ decay normal, the azimuth of deuteron in the $d\pi_1^+$ system, and even the $d\pi_1^+$ mass for non-d^* events, agree as well. It appears that this model is adequate to describe all of the features studied in the $\rho^0\pi^+d$ system, in particular the A_1, whether or not d^*'s are produced.

ACKNOWLEDGMENTS

We wish to thank Professor D. G. Ravenhall, Professor R. Schult, and R. Hicks for conversations clarifying the calculation and interpretation of models for πd scattering. The Regge-exchange model calculations were performed and interpreted with the assistance of Dr. M. Ioffredo. We thank other members of the π^+d group, in particular, Professor U. Kruse and Dr. G. Abrams, whose efforts were essential in acquiring the data presented here. The experimental run was performed with the participation of the Alvarez Group at the Lawrence Radiation Laboratory.

[9] Edmond L. Berger, Phys. Rev. 166, 1525 (1968). The calculation employs $s_0=0.8$ GeV^2 and no form factors. Only the amplitude with the $\rho\pi\pi$ vertex contributes to the matrix element.

[10] With this choice of ρ_{00}, the ρ decay angular distributions which result from the Monte Carlo are very much like the observed distributions for d^* and non-d^* events.